

MODIFICATION OF PANOBINOSTAT TO INCREASE ITS THERAPEUTIC POTENTIAL
TO CURE MULTIPLE MYELOMA

By
Sweta Adhikari

A thesis submitted to the faculty of The University of Mississippi in partial fulfilment of the
requirements of Sally McDonnell Barksdale Honors College.

Oxford
March 2017

Approved by

Advisor: Dr. Davita Watkins

Reader: Dr. Susan Pedigo

Reader: Dr. Jared Delcamp

© 2017
Sweta Adhikari
ALL RIGHTS RESERVED

ACKNOWLEDGEMENTS

I would to thank my advisor, Dr. Davita Watkins, for her continuous support and invaluable guidance through my researching. She kindly welcomed me in her laboratory and taught me how to conduct research. She patiently answered my countless questions and helped me whenever I needed her during the research. I will always be grateful for her continuous academic and emotional support during my undergraduate education.

I would like to thank Dr. Susan Pedigo and Dr. Jared Delcamp for taking the time to read my thesis and meeting me on multiple occasions.

I would also like to thank our awesome research crew for supporting me through my time in the lab. I especially want to thank you Kyra for helping me understand the research better and revising my thesis. Dr. Daniel Abebe was a great help on a daily basis to answer my innumerable questions in the lab. The whole crew always offered guidance and support throughout the process.

Last but not the least, I would like to thank the Sally McDonnell Barksdale Honors College for opportunity to challenge myself and conduct research.

ABSTRACT

SWETA ADHIKARI: Modification of Panobinostat to increase its therapeutic potential to cure Multiple Myeloma (Under the direction of Dr. Davita Watkins)

Panobinostat is a potent histone deacetylase inhibitor that can impede function of a wide range of zinc-dependent histone deacetylases. Panobinostat is the first approved histone deacetylase inhibitor for the treatment of multiple myeloma, along with other drugs such as Velcade and Dexamethasone. Simplistically, it helps to shrink or eradicate tumor growth in multiple myeloma patients. However, the treatment has severe adverse effects due to its lack of selectivity. In collaboration with Dr. Shana Stoddard (Rhodes College, Memphis TN) and Fatima Rivas (St. Jude's Research Hospital, Memphis TN), our research aims to design a more selective model of panobinostat that binds with the human histone deacetylase 8. Model compounds were examined and docking scores were computed based on protein X-ray crystal data. Herein, panobinostat derivatives having the highest docking score are presented with a synthetic scheme for the first target derivative. The synthesis and characterization by nuclear magnetic resonance (NMR) are described.

TABLE OF CONTENTS

LIST OF FIGURES AND TABLES	6
LIST OF ABBREVIATIONS.....	7
INTRODUCTION.....	8
HDAC.....	10
ROLE OF HDAC.....	11
HDACi.....	13
PANOBINOSTAT.....	14
MODIFICATION OF PANOBINOSTAT.....	15
SYNTHESIS SCHEME.....	19
FISCHER ESTERIFICATION.....	20
REDUCTION OF METHYL 5-METHYL PYRAZINE CARBOXYLATES.....	24
WITTIG REACTION.....	27
CONCLUSION.....	35
LIST OF REFERENCES.....	36

LIST OF FIGURES AND TABLES

Figure 1: Balance of acetylation and deacetylation.....	10
Figure 2: Overexpression of HDAC.....	11
Figure 3: Hypoacetylation alters the expression of genes.....	12
Figure 4: HDACi retains the balance.....	13
Figure 5: The molecular structure of panobinostat.....	15
Figure 6: Target of interest 1 (TOI1).....	17
Figure 7: The synthesis scheme to achieve TOI1.....	19
Figure 8: The mechanism of Fischer Esterification.....	21
Figure 9: ¹ H NMR of methyl 5-methyl pyrazine carboxylates.....	22
Figure 10: The mechanism of reduction reaction.....	24
Figure 11: ¹ H NMR of 5-methyl pyrazine-2-carbaldehyde.....	25
Figure 12: The mechanism of Wittig reaction.....	27
Figure 13: ¹ H NMR of Methyl (E)-3-(5-methyl pyrazine-2-yl) acrylate.....	29
Figure 14: The mechanism of formation of enamine.....	32
Figure 15: ¹ H NMR of enamine.....	33
Table 1: The docking score of various target of molecular structures.....	16

LIST OF ABBREVIATIONS

HDAC	Histone Deacetylases
HDACi	Histone Deacetylase Inhibitor
MM	Multiple Myeloma
DNA	Deoxyribonucleic acid
HAT	Histone Acetyltransferases
TOI	Target of Interest
RBF	Round Bottom Flask
NMR	Nuclear Magnetic Resonance spectroscopy
DCM	Drychloromethane
RT	Room Temperature
DIBALH	Di-isobutyl Aluminum Hydride
Aq.	Aqueous
g	grams
mL	milli liters

INTRODUCTION

Cancer is a collection of illnesses that involves the uncontrollable growth of abnormal cells that have the ability to spread to surrounding tissues within the body. When abnormal cells divide, they form tumors that can either be benign (non-cancerous) or malignant (cancerous). In this discussion, we will primarily focus on malignant plasma cells that causes multiple myeloma (MM).

In our immune system, lymphocytes are the most important cells that fight infections and other diseases¹. T cells and B cells are two major types of lymphocytes. B cells bind to the antigen and receives a signal from T cells to divide. The B cells continuously divide and eventually transform into plasma cells. Plasma cells, located in bone marrow, produce antibodies that kill germs and other infections within the body. When the plasma cells become cancerous, they divide rapidly and form a tumor or *plasmacytoma* in the bone. The cancer associated with the formation of more than one tumor in the bone is known as MM. It can lead to fewer white blood cells, infections, weaker bones, and kidney problems among other complications.

MM is found to be an outstanding example of epigenomics dysregulation in human body because epigenetic aberrations play an important role in the development of MM². Epigenetics refers to the complex interactions between the genome and the environment that leads to growth and regulation in the body³. For the regulatory patterns of gene expression, epigenetic modification occurs such as DNA methylation and posttranslational histone modification². There are high levels of epigenetic modifications in the cancer cells that transform the chromatin structure and DNA accessibility³.

One of the most highly studied epigenetic modifications in MM is the histone modification². The overexpression of histone deacetylase (HDAC) leads to hypoacetylation of histones in cancer

cells, resulting in cell survival and multiplication. Aforementioned reasons have led to synthetic study of HDAC inhibitors (HDACi) to examine if they help reduce the size of MM tumors. Panobinostat is a pan-HDACi that shows a great potential to cure MM, but due to its lack of selectivity causes various adverse effects in majority of patients.

With the hope of developing a better therapeutic treatment, researchers are seeking the development of HDACis with high potencies and efficiencies. With the help of our colleagues at Rhodes College and St. Jude's Research Hospital, we were able identify several target molecules that show properties that are comparable to those of a leading HDACi known as panobinostat. Specifically, our lab contributes to the study by offering synthetic strategies towards these molecules. Herein, a brief background pertaining to the role of HDAC and HDACis is discussed. In addition, the synthesis of a panobinostat derivative (TOI) is described in an effort to further study its therapeutic applications.

BACKGROUND

1. HDAC

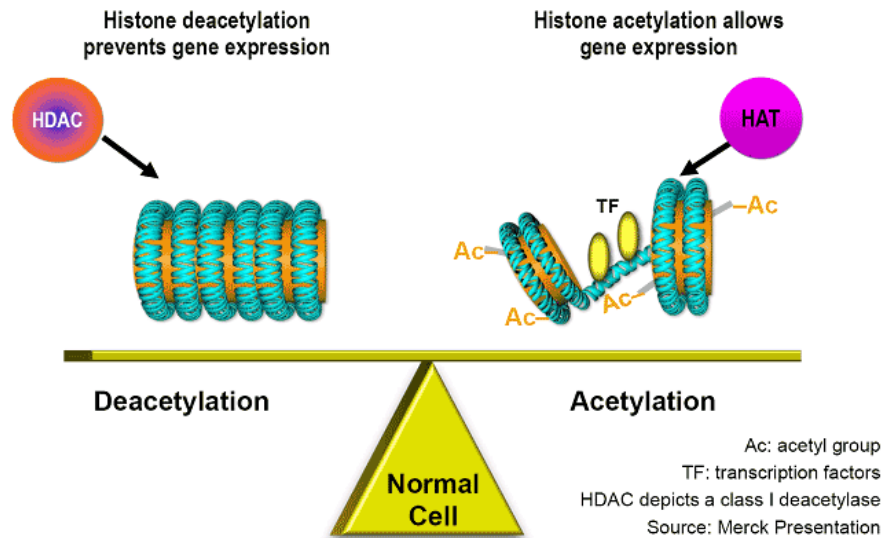


Figure 1: Equilibrium of acetylation and deacetylation during transcription in a normal cell.¹⁴

Typically, during the activation of transcription, acetyl groups are added to an amino acids on histones in the DNA by the enzyme histone acetyltransferases (HATs) to form active chromatin⁷. However, HDACs removes acetyl groups from an amino acid on the histone, to control the turning on and off of genes during transcription as shown in Figure 1.

There are four classes of histone deacetylase; class I (HDAC1, HDAC2, HDAC3, HDAC8), class II (HDAC 4, HDAC 5, HDAC 6, HDAC 7, HDAC 9, HDAC 10), class III (Sirtuin proteins), and class IV (HDAC 11)¹⁷. Except for class III, all the HDAC require zinc as a cofactor, therefore they are known as zinc dependent HDACs. Class III enzymes are considered a separate type of NAD⁺ dependent enzymes and have a different mechanism of action¹⁶.

2. Role of HDAC in cancer

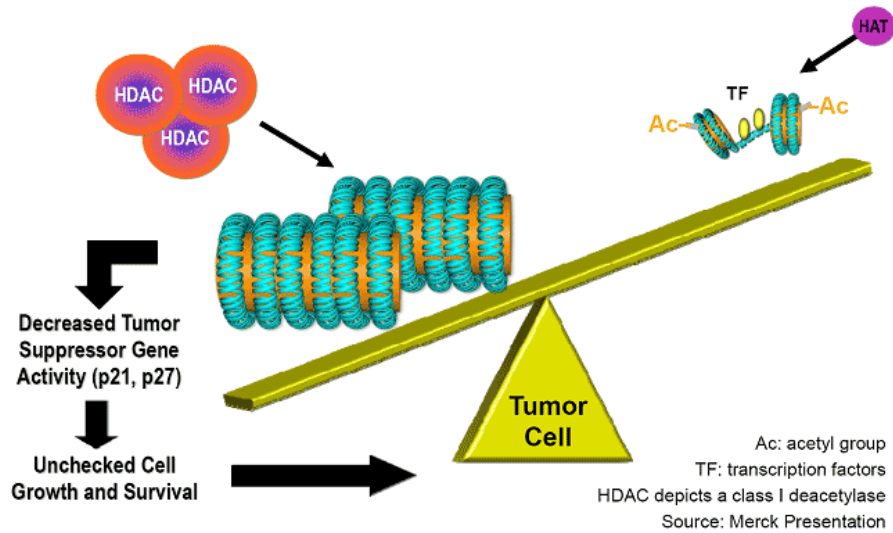


Figure 2: Overexpression of HDAC leads to hypoacetylation in cancer cells.¹⁴

A typical characteristic of human cancer is the dysregulation of posttranslational histone modification, specifically histone acetylation⁷. Due to epigenetic modifications, there is a decrease in HAT activity and increase in HDAC activity. When HDACs are overexpressed, the tumor suppressor genes are repressed during the onset and progression of tumor. It causes unregulated cell growth and survival as shown in Figure 2.

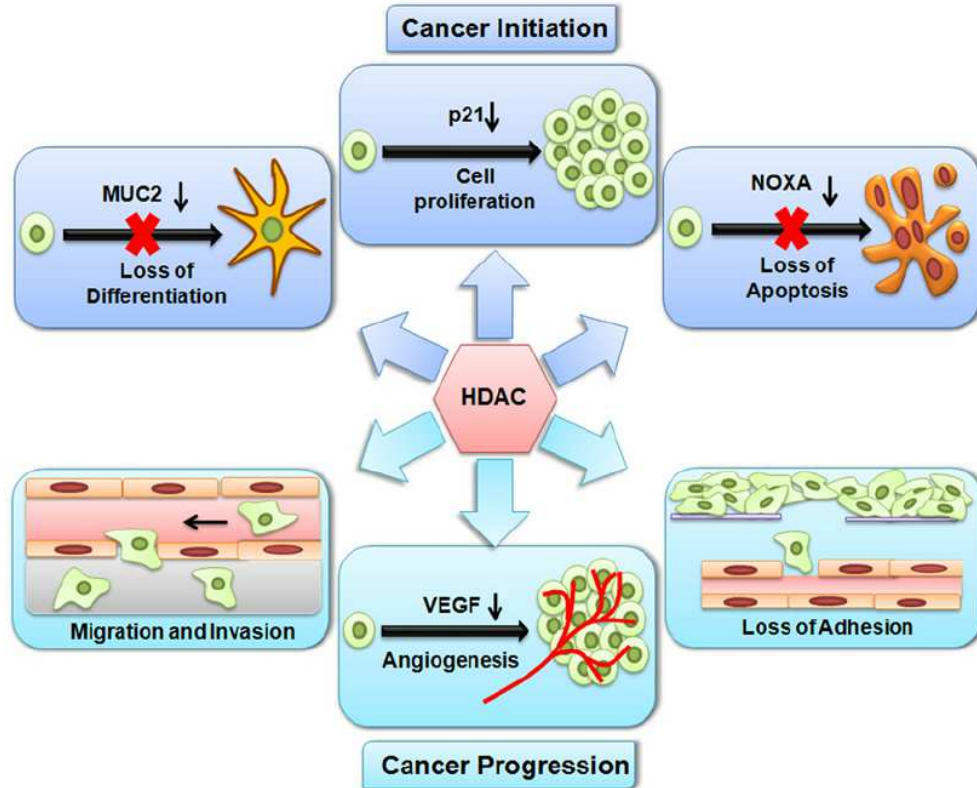


Figure 3: Hypoacetylation alters the expression of genes causing cancer initiation and progression.¹⁵

HDAC alters the expression of tumor suppressing genes and favors the development of cancer¹⁵. HDAC represses genes resulting in the uncontrolled cell proliferation, loss of differentiation, and inhibition of apoptosis. Similarly, during cancer progression, HDAC represses genes, resulting in a loss of adhesion, migration, invasion, and angiogenesis. Loss of intercellular adhesion allows malignant cells to escape from their site of origin and metastasize. Also, there is new growth in the vascular network for adequate supply of oxygen and nutrients and removal of waster products for cancer cells through a process called angiogenesis.

3. HDACi

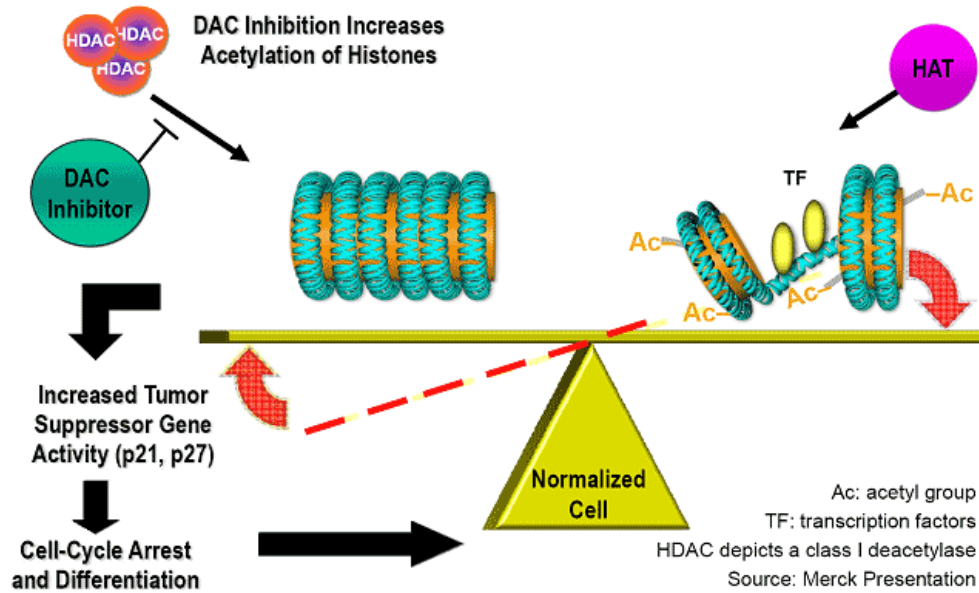


Figure 4: HDACi retains the balance between acetylation and deacetylation.¹⁴

HDACi induces acetylation of histones in the cancer cells and increases tumor suppressor gene activity. This phenomenon results in cell cycle arrest, differentiation, or apoptosis to inhibit the proliferation of cancer cells⁴.

HDACi have been extracted from natural products or synthesized in the laboratory. Pan-HDACi is an HDAC inhibitor that has been approved as a drug which acts broadly on all forms of zinc- dependent HDACs¹⁶. A few examples of pan-HDACi are trichostatin A, vorinostat, and panobinostat. However, with the treatment of HDACi, normal cells were found to be quite resistant. In our research, we are concentrating on panobinostat, which induces wide range of HDACs.

4. Panobinostat

Panobinostat is a potent oral pan-HDACi that has shown high therapeutic potential in its ability to inhibit a wide range of HDACs including classes I, II, and IV at nanomolar concentrations⁵. It uses metal-ion coordination to bind with the zinc ion in histone. Thus, it can inhibit the zinc-dependent HDACs because of its binding capabilities and selectivity. It is the first HDACi approved for the treatment of MM with the combination of other drugs such as velcade and dexamethasone in 2015^{8,9}. Velcade is a brand name of the drug bortezomib that interferes with the growth of some cancer cells and keeps them from spreading in your body. Similarly, dexamethasone is a drug that reduces swelling and inflammation.

In a clinical trial referred to as PANORAMA1, 193 patients were randomly appointed to receive either combination of three drugs: panobinostat, bortezomib, and dexamethasone, or combination of two drugs (placebo): bortezomib and dexamethasone⁸. These patients had already received previous treatments, or did not respond to the treatments. During the treatment, the cancer had reduced or disappeared in 59% of the patients with the combination of panobinostat in comparison to the other 41% without panobinostat. However, 96% of the patients treated with panobinostat experienced side effect such as nausea, vomiting, diarrhea, fatigue, and thrombocytopenia (deficiency of platelets in the blood) among which 60% experienced far more serious side effects⁶. The median of progression free survival was 10.6 months with panobinostat and 5.8 months without it. With the hope of developing a better therapeutic treatment, researchers are seeking the development of HDACis with potencies and efficiencies that are similar to that of panobinostat.

RESULTS AND DISCUSSION

5. Modification of Panobinostat

In collaboration with colleagues at Rhodes College and St. Jude's Research Hospital, we were able to identify several target molecules that show properties that are comparable to that of panobinostat.

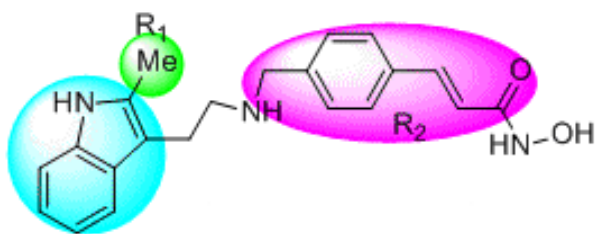
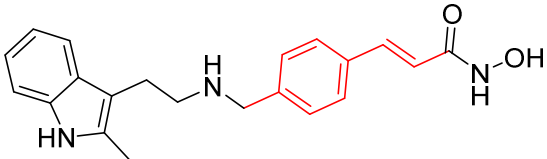
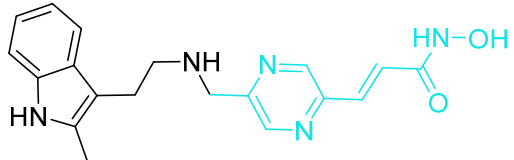
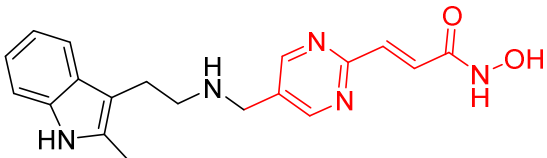
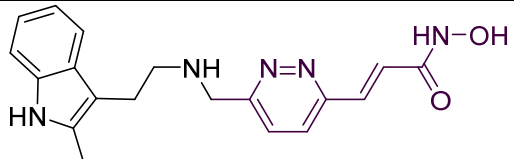
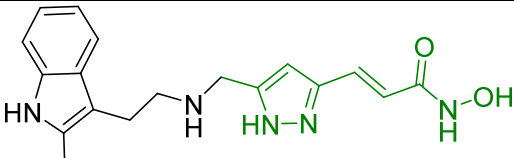
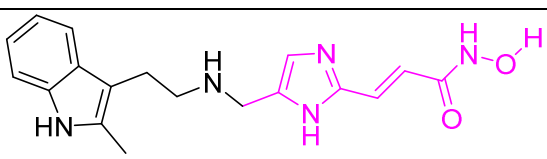


Figure 5: Molecular structure of panobinostat

In order to study and model several target molecules, the molecular structure of panobinostat was divided into four regions. The blue region is an indole, which cannot be changed in the target molecules because it is necessary for protein binding and recognition. N-hydroxyl amine is necessary for binding with zinc in histones. In turn, the two regions for interest towards alteration and study are the green alkyl group ($R_1 = \text{methyl}$) and the purple amino methyl phenyl prop-2-enamide region.

The focus of our studies was based on the identification of molecular interactions between panobinostat and the protein present in histone human HDAC8. In this case, the noncovalent interactions between the protein and panobinostat derivative are pi-pi stacking and hydrogen bonding. Computational studies based on protein X-ray crystal data were used to find the docking scores of the model compounds. Docking scores are mathematical methods used to predict the

strength of non-covalent interaction between two molecules after they have been docked. Docking of protein is done to predict the position and orientation of a ligand when it is bound to a protein receptor. It can be done by X-ray crystallography to visualize protein structures at the atomic level and understand the how proteins interact with other molecules.

Docking Scores of Targets of Interests		
Compound	Best Docking Score	Structure
PANO	9.3381	
TOI1	10.2300	
TOI2	9.5874	
TOI3	8.8060	
TOI4	9.4581	
ETS1	9.4565	

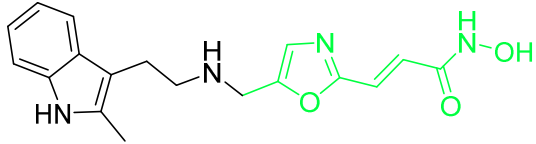
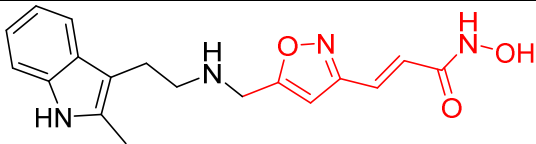
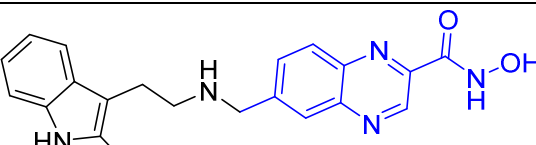
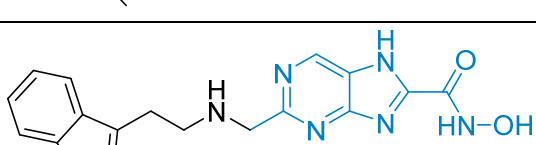
ETS2	8.9591	
ETS3	8.8402	
ETS4	8.7114	
ETS5	8.6623	

Table 1: The docking scores of various molecular structures having organic frameworks similar to panobinostat were calculated based on protein X-ray crystal data using SYBYL-x Surflex DOCK program.

From the results from Table 1, we can see the rank of docking score of compounds in increasing order is **TOI1** (10.2300) > **TOI2** (9.5874) > **TOI4** (9.4581) > **ETS1** (9.4565) > **PANO** (9.3381) > **ETS2** (8.9591) > **ETS3** (8.8402) > **TOI3** (8.8060) > **ETS4** (8.7114) > **ETS5** (8.6623).

Based on the data, we began to synthesize (E)-N-hydroxy-3-[4-[[2-(2-methyl-1H-indol-3-yl)ethylamino]methyl]pyrazine]prop-2-enamide-referred to as **TOI**, which outcompeted **PANO** suggesting a strong potential to be an HDACi.

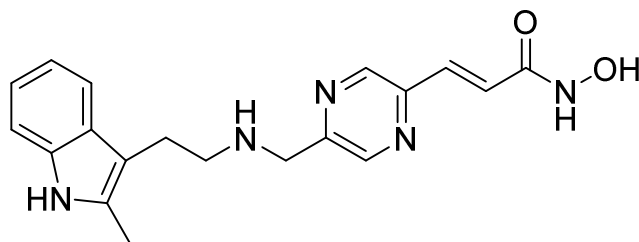


Figure 6: Target of interest 1 (TOI1) having the highest docking score, one which is greater than that of panobinostat.

The alteration in the structure of TOI is a replacement of a pyrazine instead of a benzene ring. Pyrazine contributes to increased selectivity in binding with human histone HDAC, avoiding unintended consequences. Our lab contributes to the study by offering synthetic strategies towards these molecules. Herein, the synthesis of a panobinostat derivative (TOI) is described in an effort to further study its applications.

6. Synthesis Scheme

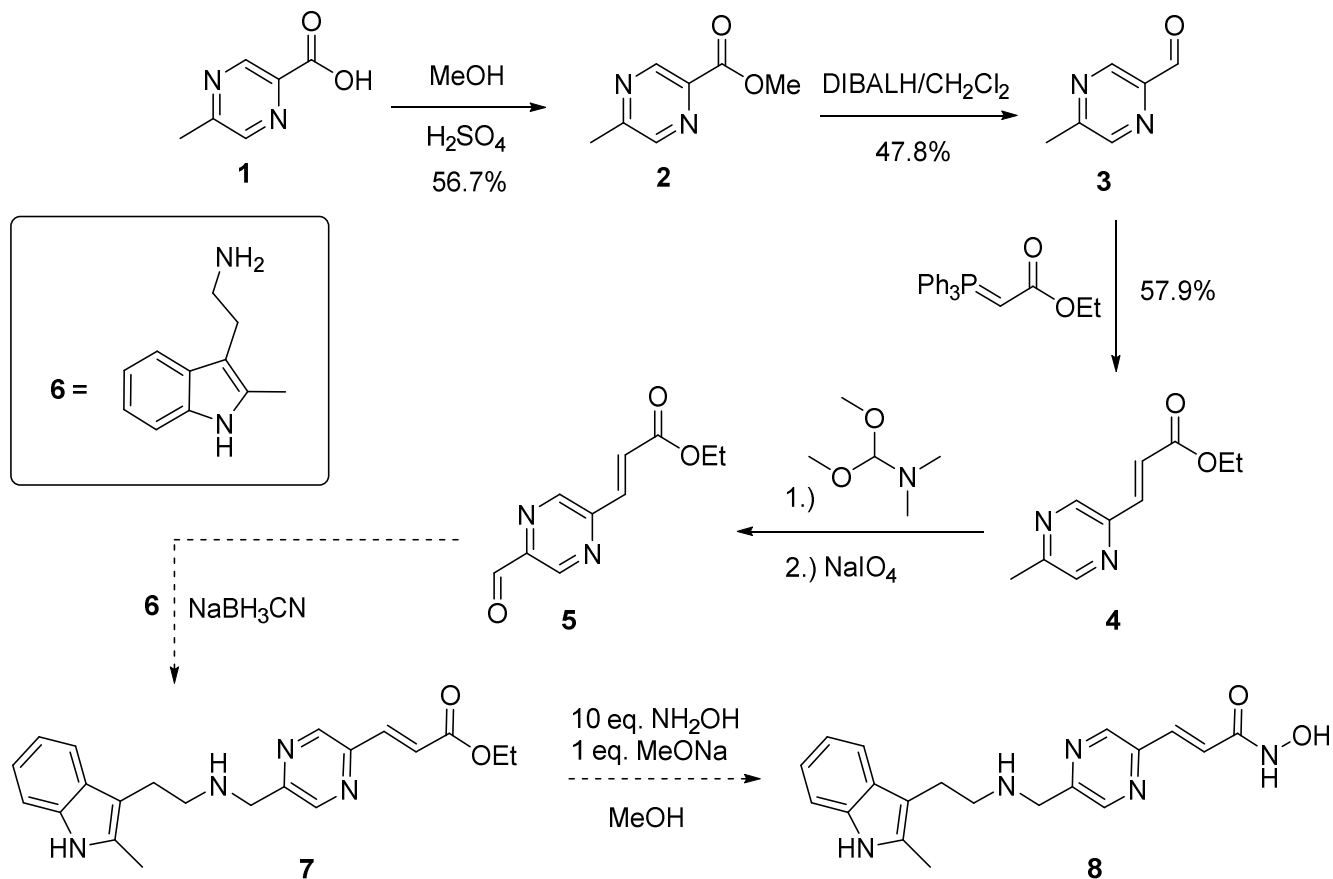
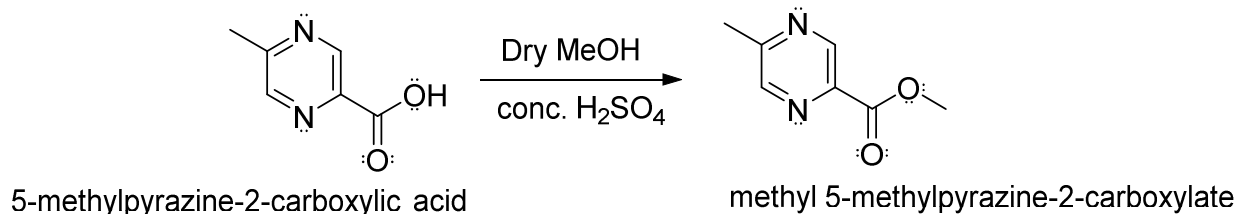


Figure 7: The synthesis scheme to achieve TOI1.

In the synthesis scheme, the first step is Fischer esterification of carboxylic acid. Then, the ester is reduced to aldehyde in the second step. The third step is the Wittig reaction to synthesize acrylate. The formyl group is added to the acrylate in the fourth step. Then, the Borch reductive amination is done in the sixth step to add the indole amine to the acrylate. Finally, the ester in the acrylate is converted to N-hydroxyl amine to achieve TOI1.

7a. Fischer Esterification of 5-methyl pyrazine carboxylic acid



Mechanism:

Fischer esterification is the esterification done by refluxing a carboxylic acid and an alcohol in the presence of an acid catalyst. The electrophilic nature of the carbonyl carbon and the nucleophilic nature of the alcohol results in the nucleophilic acyl substitution. The water formed in the reaction is very likely to hydrolyze the ester, therefore the addition of a molecular sieve to the reaction mixture was very important to absorb water.

As shown in Figure 8, during the esterification, the proton transfer from the sulfuric acid to the carbonyl oxygen increases electrophilicity of the carbonyl carbon. Then, the nucleophilic oxygen atom of the methanol attacks the carbonyl carbon. The proton from the oxonium ion attached to the methyl group is transferred and creates water, which leaves the complex creating a new oxonium ion. Finally, deprotonation of the oxonium ion gives the final ester.

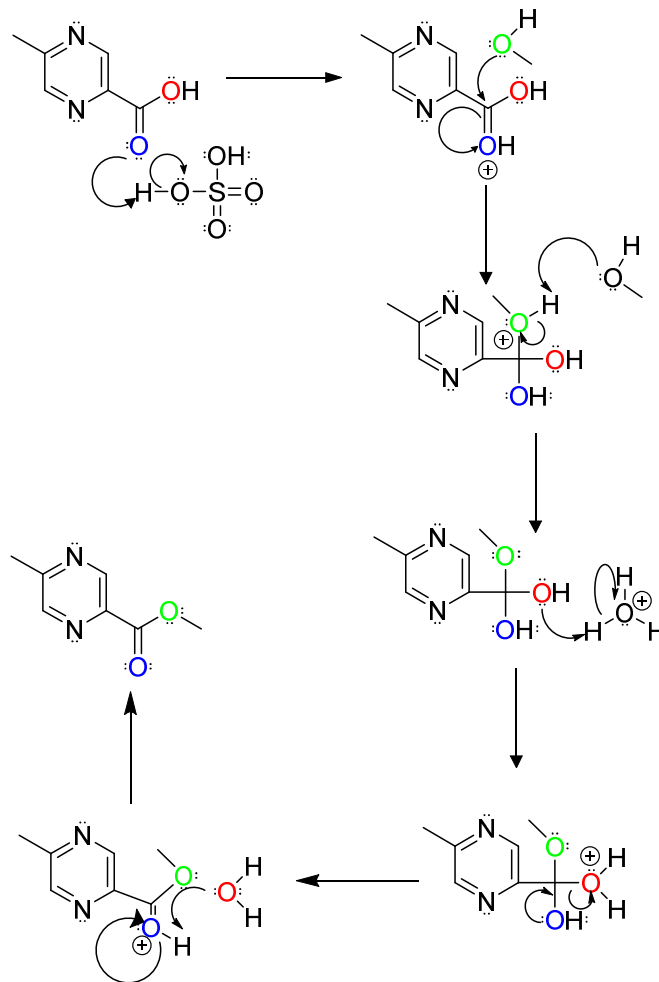


Figure 8: The mechanism of Fischer esterification of 5-methyl pyrazine carboxylic acid to produce methyl 5-methyl pyrazine carboxylate.

Procedure:

To a three neck 500 mL round bottom flask (RBF), 2.75 g of molecular sieve was measured and added along with a stir bar. The RBF was flamed dried to create an inert environment. Then, 5 g of 5-methyl pyrazine carboxylic acid was added in the RBF. The RBF was degassed and gassed several times to rid the reaction vessel of air. A volume of 125 mL of anhydrous methanol was added to the flask and stirred for few minutes. Slowly, 91 drops of glacial sulfuric acid was added of the mixture. The reaction was allowed to stir and reflux overnight¹¹.

Extraction:

Molecular sieve was filtered off via vacuum filtration through celite. The filtrate was evaporated to remove methanol from the product. The product was dissolved in DCM, and washed with brine and sodium bicarbonate in a separatory funnel. The organic layer was collected and dried over sodium sulfate. The solvent was then evaporated to obtain the product.

NMR:

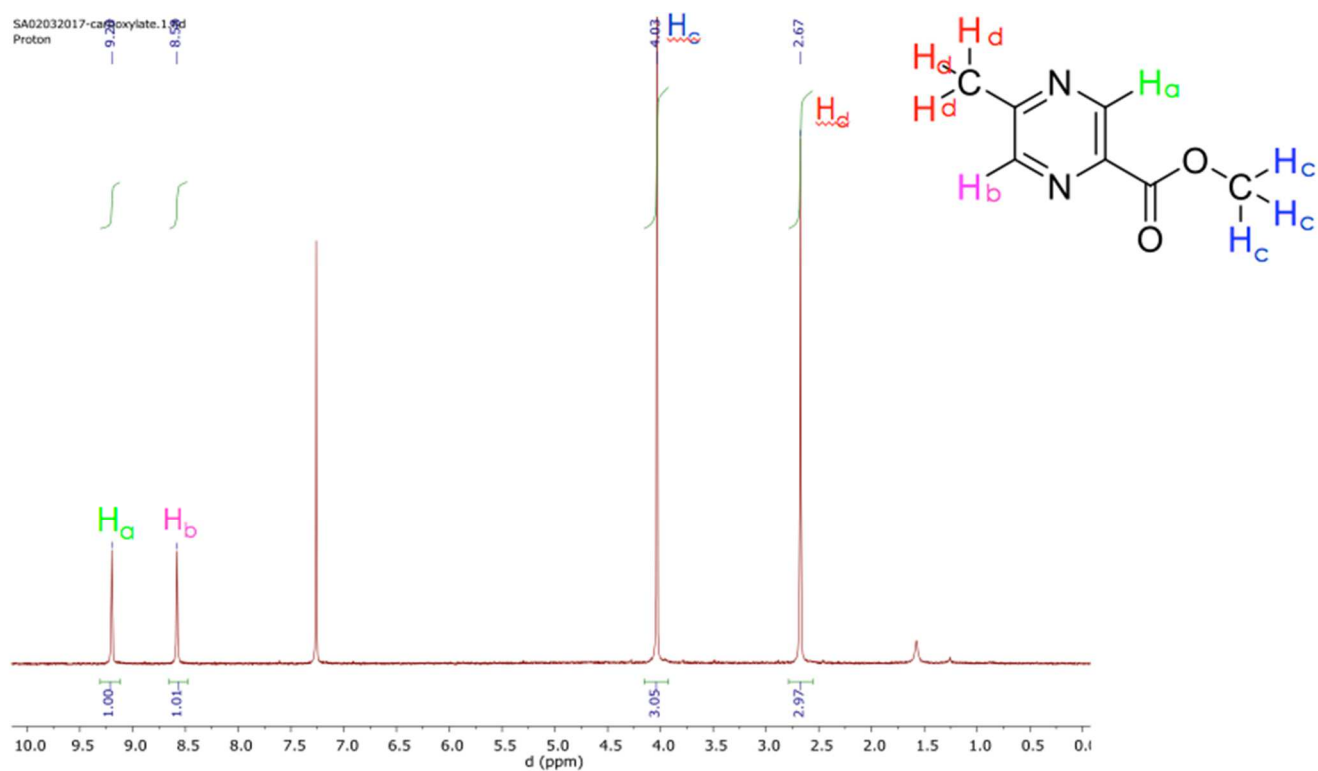


Figure 9: ¹H NMR of methyl 5-methyl pyrazine carboxylates - (300 MHz, CDCl₃) δ 9.29 (1H, s), 8.58 (1H, s), 4.03 (3H, s), 2.67 (3H, s)

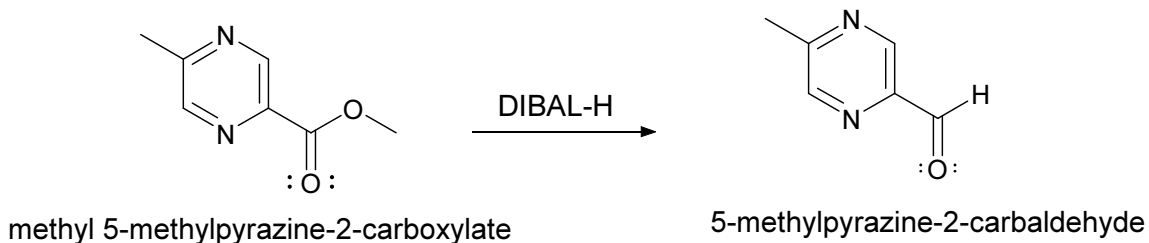
Result:

The weight of the solid yellow colored sample was 3.08 g. The yield was calculated to be 56.7%.

Discussion:

The ^1H NMR spectra was recorded on a 300 MHz instrument using CDCl_3 solvent. In the spectrum, there are two singlets at 9.29 ppm and 8.58 ppm which belong to the two proton signals in the aromatic pyrazine ring. The peak at 9.29 ppm belongs to the proton signal (H_a) near the carbonyl, whereas the peak at 8.58 ppm belongs to the proton signal (H_b) near methyl group. The singlet at 4.03 ppm belongs to the proton signal (H_c) in the methoxy group of the ester. The singlet at 2.67 ppm belongs to the proton signal (H_d) for the in methyl group on the pyrazine ring. Thus, we concluded that we produced the desired ester.

7b. Reduction of methyl 5-methyl pyrazine carboxylates



Mechanism:

In the mechanism of the reaction, DIBAL-H acts as an electrophilic reductant. In the first step, the nucleophilic lone pair of carbonyl oxygen attacks the electrophilic aluminum in DIBAL-H and the DIBAL-H then provides the hydride to the carbonyl oxygen forming the tetrahedral intermediate. Then, the methoxy group leaves the intermediate to generate negative charge on O in

the leaving group and positive charge on O bonded to Al. Then, the methoxy group attacks Al forming the aldehyde.

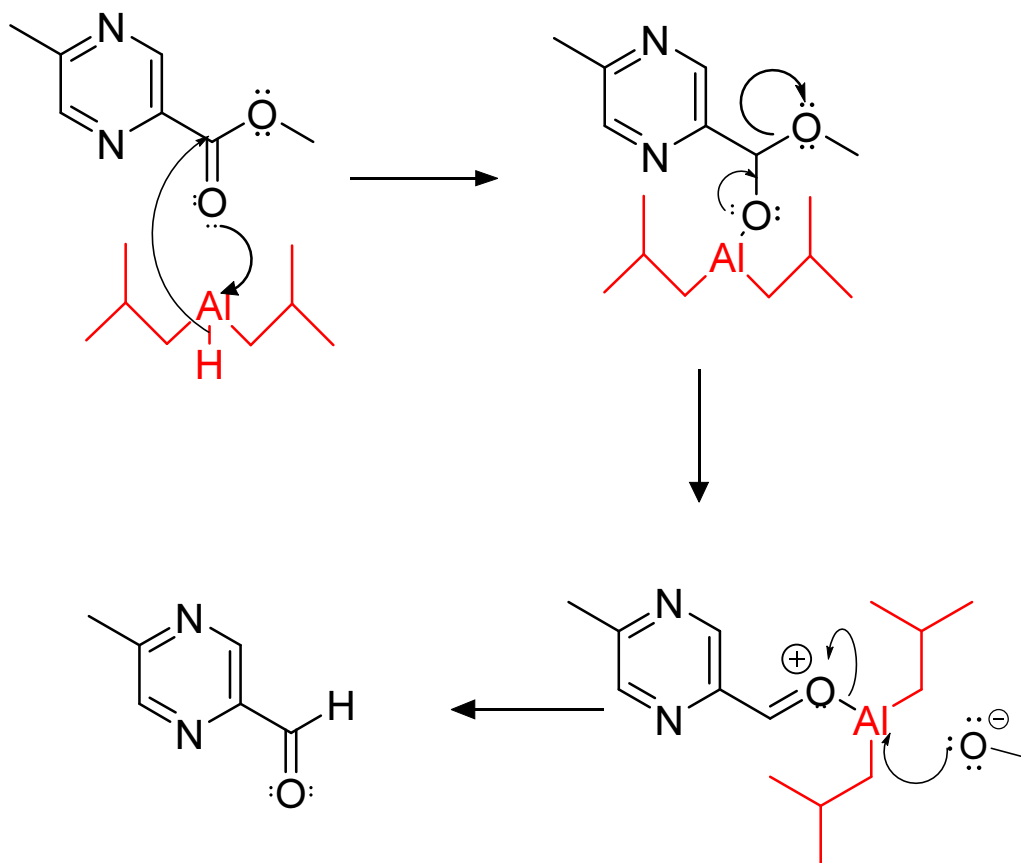


Figure 10: The mechanism of Reduction Reaction of methyl 5-methyl pyrazine carboxylate to produce 5-methyl pyrazine-2-carbaldehyde.

Procedure:

Under dry and inert conditions, 1.06 g of methyl 5-methyl pyrazine carboxylate was added to the round bottom flask. Then, 10 mL of dry DCM was added to the RBF. The reaction was placed in ice bath to reduce the temperature to -78°C . After the reaction reached -78°C , 10 mL of DIBAL-H was added¹². The reaction was allowed to stir for three hours.

NMR:

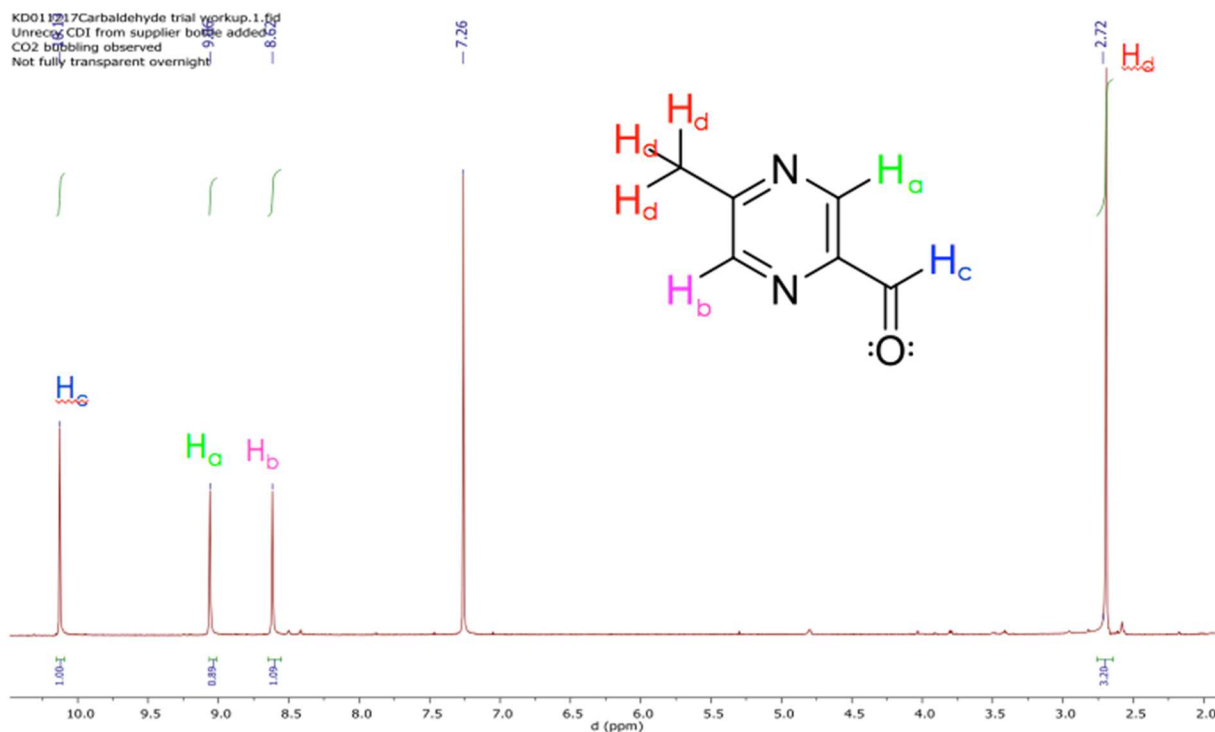


Figure 11: ^1H NMR of 5-methyl pyrazine-2-carbaldehyde (300 MHz, CDCl_3) δ 10.13 (1H, s), 9.06 (1H, s), 8.62 (1H, s), 2.72 (3H, s)

Result:

The oily brown crude weighed 4.4133g. The yield was considered 100%, solvent was removed and crude was used as obtained.

Discussion:

In the reduction reaction, DIBAL-H is used to reduce ester to aldehyde. In the reaction, the temperature was maintained around -78°C to prevent the further reduction to alcohol. To monitor the course of the reaction and the formation of aldehyde, DIBAL-H was added in small aliquots. After the reaction reached -78°C , 5 mL of DIBAL-H was added. The reaction was allowed to stir

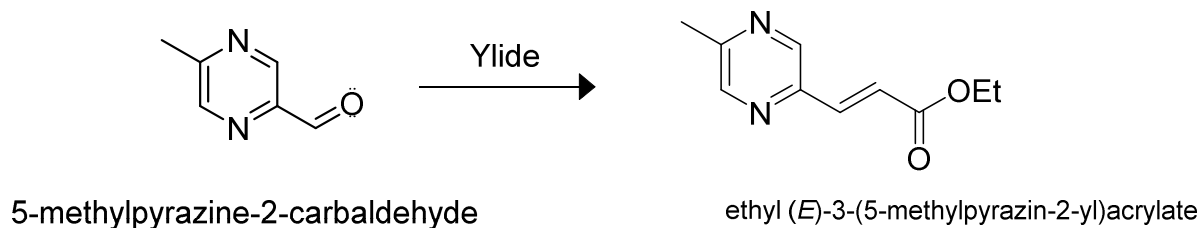
for an hour. A 2.5 mL solution of DIBAL-H was added to the mixture and stirred for another hour. Finally, 2.5 mL of DIBAL-H was added and the reaction was let stir for 1 hour.

Also, the aqueous workup of the crude was avoided in this experiment since the workup always favored the hydrate formation and produced very low yield of the aldehyde. In presence of acid media (work-up), an aldehyde can form an aldehyde hydrate. Although, the aldehyde hydrate may be present in low equilibrium concentration, those molecules bearing an electron withdrawing group (e.g. pyrazine) can yield stabilized hydrates (not shown, ^1H NMR signals at 5.49 and 4.72 ppm). Therefore, the aqueous work up was avoided and the crude was evaporated and used in the next step.

The ^1H NMR spectrum was recorded on a 300 MHz instrument using CDCl_3 solvent. The singlet peak at 10.13 ppm belongs to the proton signal (H_c) in the aldehyde. This peak confirms the presence of aldehyde in the product. The singlet peak at 9.06 ppm belongs to the proton (H_a) in the aromatic ring near carbonyl compound. The singlet at 8.62 ppm belongs to the proton (H_b) in the aromatic region near the methyl group. The singlet at 2.72 ppm belongs to the proton (H_d) in methyl group.

Although we had complication regarding the aqueous workup, we were successful at obtaining the aldehyde.

7c. Wittig Reaction



Mechanism:

Wittig reaction is a reaction of an aldehyde and ylide to form an alkene product and triphenyl phosphine oxide byproduct. The mechanism includes the nucleophilic addition of the ylide to the electrophilic carbonyl group forming the four membered ring. Then, the ring collapses to form a strong O=P bond and an alkene bond due to ring strain and stable O=P bond.

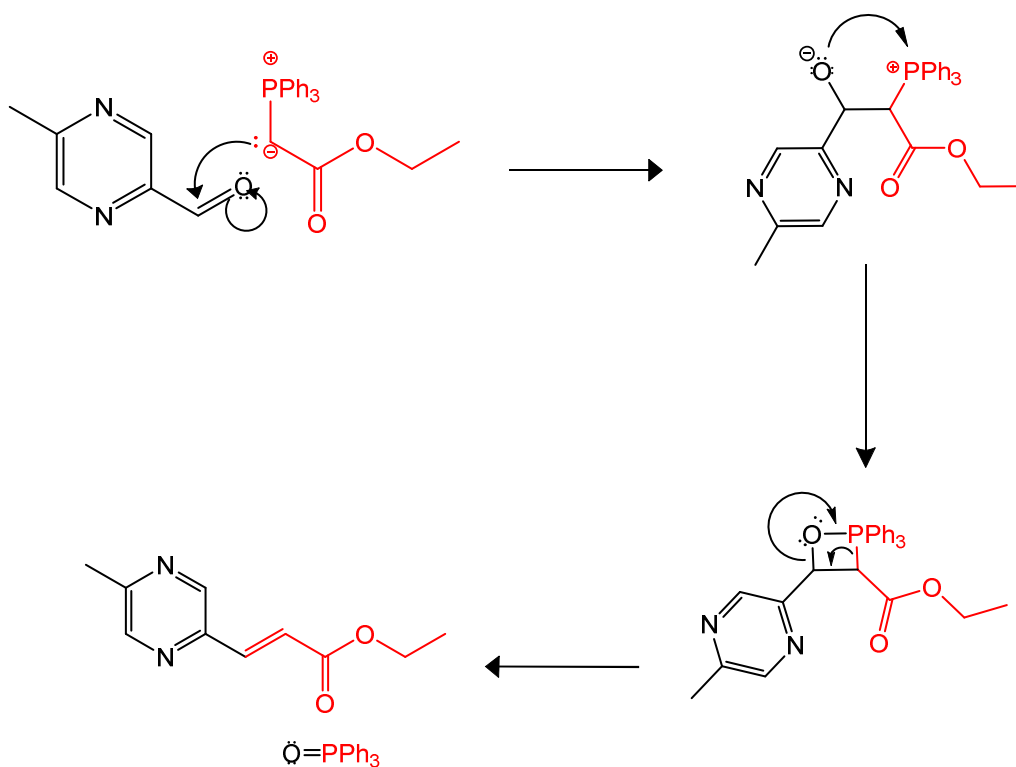


Figure 12: The mechanism of Wittig reaction of 5-methyl pyrazine-2-carbaldehyde to synthesize ethyl (E)-3-(5-methyl pyrazine-2-yl) acrylate.

Procedure:

In a dry and inert atmosphere, 1.39 g of ethoxy carbonyl methylane triphenyl phosphorene (ylide) and 20 mL of DCM was added to the round bottom flask. The remaining 20 mL of DCM was used to dissolve 0.5 g of carbaldehyde in a separate RBF. The RBF was then put in the dry ice bath to

decrease the temperature to -78°C . After the RBF was at -78°C , the carbaldehyde solution was transferred to the RBF through a cannula. Then the reaction ran at -78°C for 10 minutes. After that, the reaction ran for 1 hour at RT¹³.

Extraction:

After the reaction was done, the crude was quenched in aq. ammonium chloride and washed with brine in a separatory funnel. The organic layer was extracted and dried in anhydrous magnesium sulfate. The acrylate was obtained after the solvent was evaporated. The NMR revealed a lot of impurities in the product. Thus, the product was purified via column chromatography.

Purification:

The column was done using a 50:50 hexane and ethyl acetate solution. Acrylate eluted in the first few test tubes. The bright yellow acrylate solution was evaporated.

NMR:

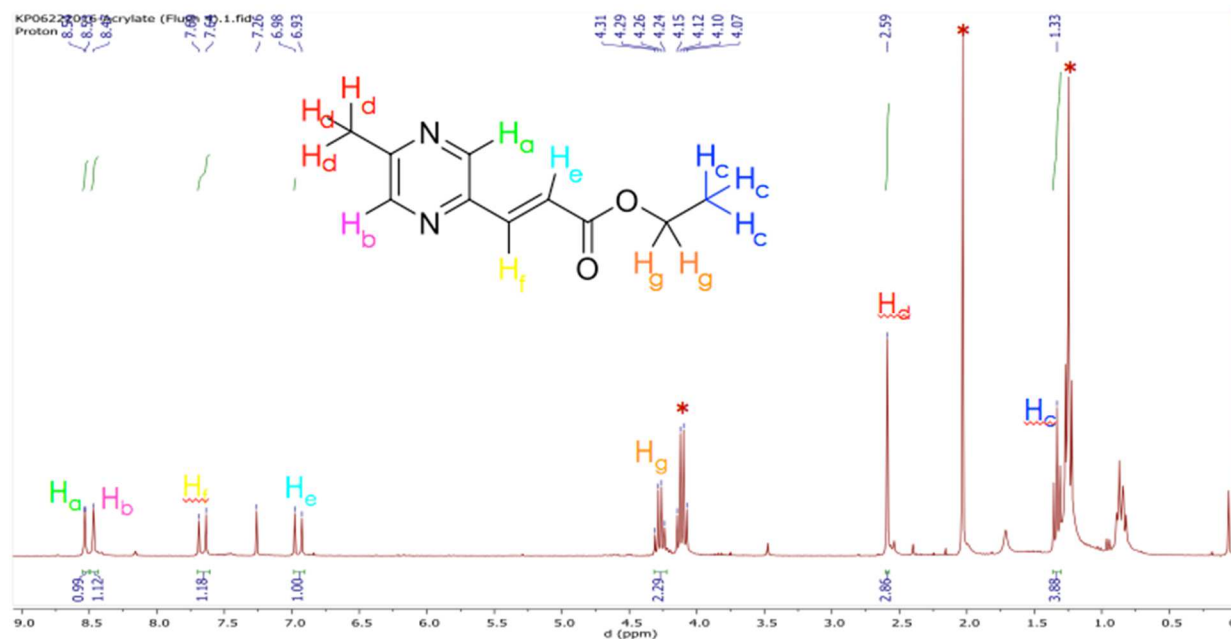


Figure 13: ¹H NMR of Ethyl (E)-3-(5-methyl pyrazine-2-yl) acrylate (300 MHz, CDCl₃) δ 8.54 (1H, s), 8.49(1H, s), 7.64-7.69 (1H, d), 6.93-6.98 (1H, d), 4.24-4.31 (2H, q), 2.59 (1H, s), 1.31-1.33 (3H, t); *solvent impurity: ethyl acetate

Result:

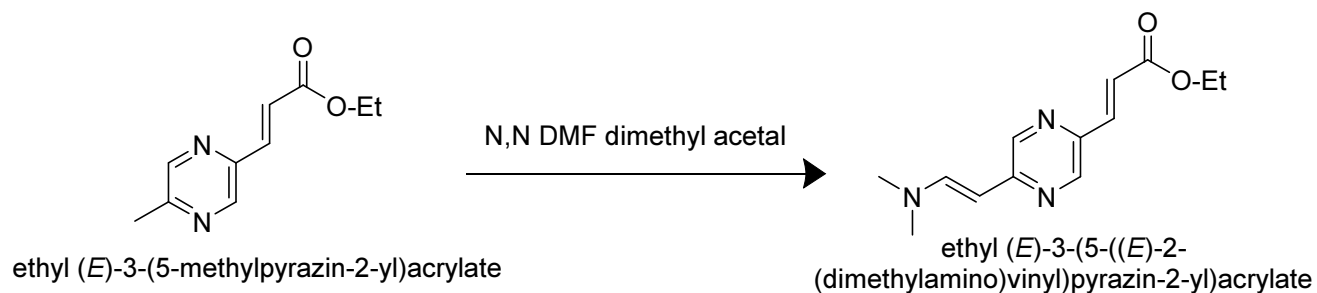
The final weight of yellow solid crystals was 0.44 g. The percent yield was 57.9%. The stereochemistry of the alkene product was trans (E) based on the coupling constant for the alkene proton signal.

Discussion:

The ¹H NMR spectra was recorded on a 300 MHz instrument using CDCl₃ solvent. The singlet peak at 8.54 ppm belongs to the proton signal (H_a) in the pyrazine ring near the alkene group. The singlet peak at 8.49 ppm belongs to the proton signal (H_b) in the pyrazine ring near methyl group. The doublet at 7.64-7.69 ppm belongs to the proton signal (H_f) in in the alkene group next to the

pyrazine ring. The doublet at 6.93-6.98 ppm belongs to the proton signal (H_e) in the alkene group next to the carbonyl group. The ylide used in the reaction is very stable, thus it favors a particular stereochemistry of the product. The j - j coupling constant for the alkene proton signal was calculated to be 16, which confirms that the stereochemistry of the product is *trans*. The quartet at 4.24-4.31 ppm belongs to the proton (H_g) in methyl group of the ester. The singlet (H_d) at 2.59 ppm belongs to methyl group on the pyrazine ring. Also, the triplet at 1.31-1.33 ppm belongs to the methylene group (H_c) of the ester. In conclusion, we successfully obtained acrylate from the aldehyde by the Wittig reaction.

7 d. Synthesis of ethyl (*E*)-3-(5-((*E*)-2-(dimethyl amino) vinyl) pyrazine-2-yl) acrylate



Mechanism:

The nucleophilic methoxy ion is formed during the equilibrium of *N,N*-dimethyl formamide dimethyl acetal. It attacks the proton in the methyl group on the pyrazine, making the methyl anion nucleophilic. The methyl anion then attacks the imine derivative. Finally, the double bond forms due to the loss of methoxy group to form ethyl (*E*)-3-(5-((*E*)-2-(dimethyl amino) vinyl) pyrazine-2-yl) acrylate.

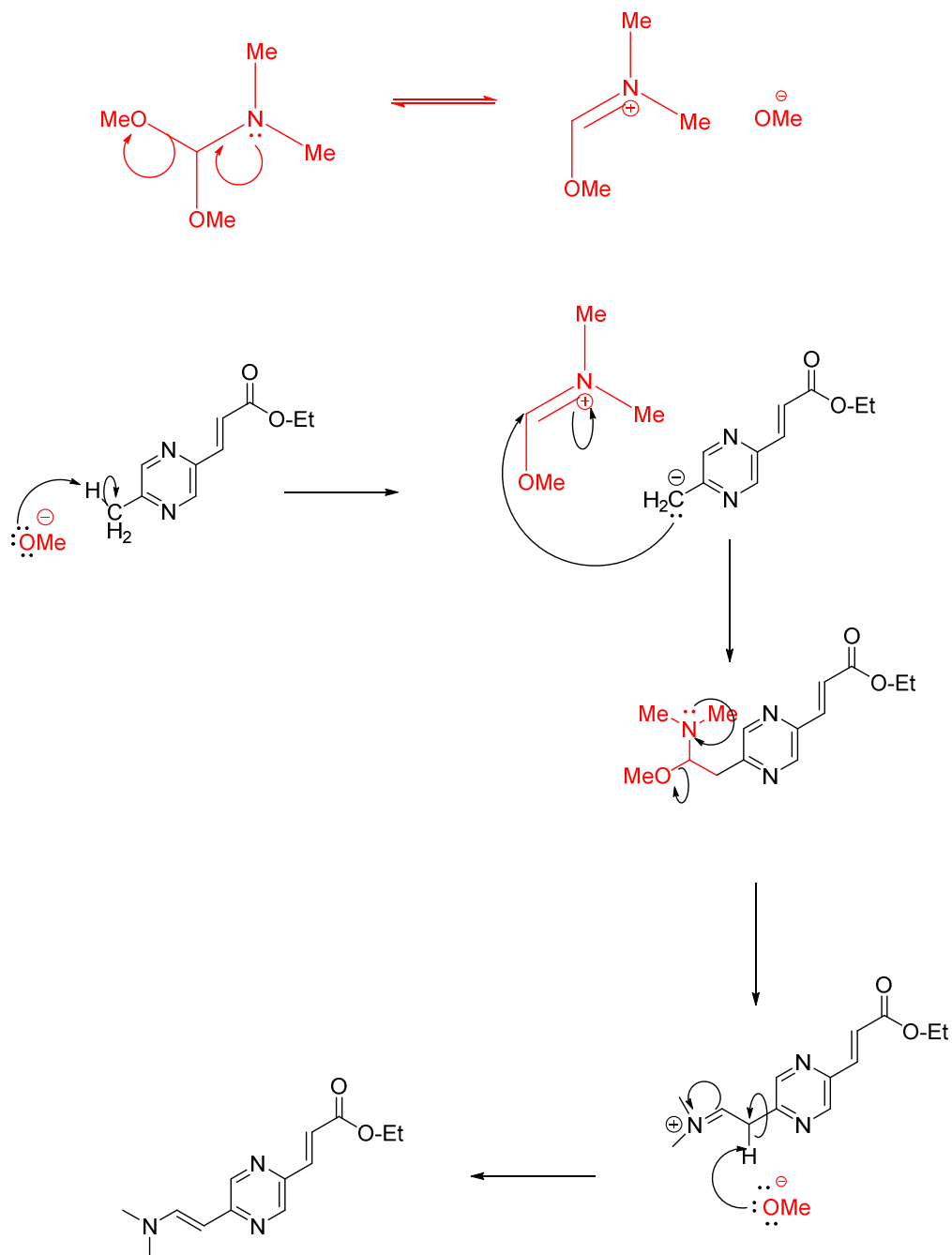


Figure 14: The mechanism to synthesize ethyl (E)-3-(5- ((E)-2-(dimethyl amino) vinyl) pyrazine-2-yl) acrylate (enamine).

Procedure:

Under dry and inert atmosphere, 0.64g of acrylate, 1.75 mL N, N dimethyl formamide dimethyl acetal, and 2 mL anhydrous N,N-dimethyl formamide was added to 50 mL RBF. The reaction

mixture was heated to 90 °C for an hour. Then, the reaction mixture was heated at 125 °C for two hours. The reaction mixture was cooled to 25 °C.

NMR:

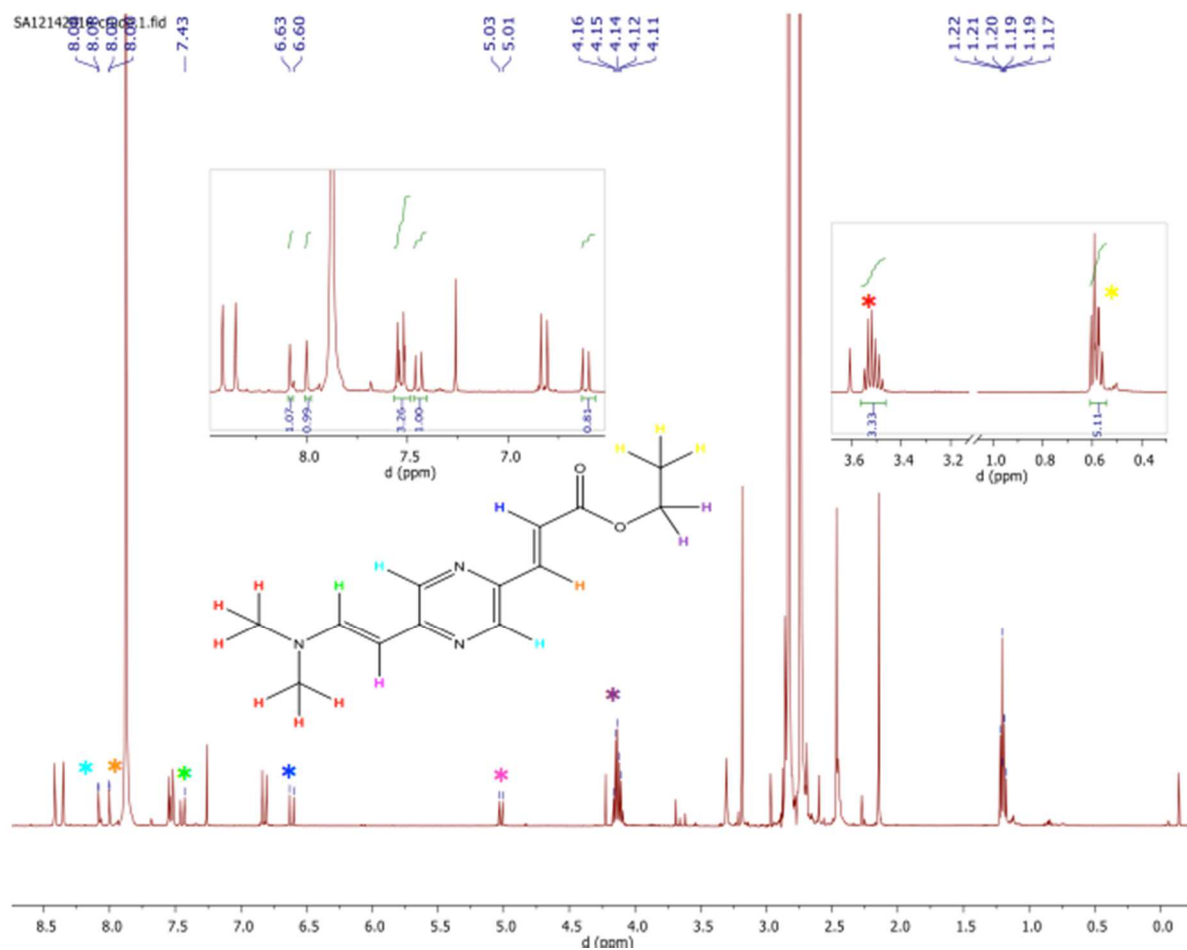


Figure 15: ¹H NMR of ethyl (E)-3-(5-((E)-2-(dimethyl amino) vinyl) pyrazine-2-yl) acrylate * (300 MHz, CDCl₃). Solvent impurities- DMF and starting material

Result:

The reaction was only 35% complete according to ¹H NMR data.

Discussion:

In the NMR, we can see the presence of the product shown by the asterisks as well as starting material and the solvent, DMF. The peak assignments are not conclusive however, the product was appears to be 35% of the reaction mixture monitored over several days. In the future, we plan to run the reaction at a higher temperature and for longer period of time. If the reaction does not go forward, we will seek an alternative reaction.

CONCLUSION

Panobinostat shows high therapeutic potential to cure multiple myeloma. However, due to the lack of selectivity, it often produces unwanted consequences. Since it is a potential drug, our colleagues at Rhodes College studied and designed a derivative of panobinostat, which has better docking score than panobinostat itself. We then designed a multi-step synthetic route to synthesize the target. Among the seven steps, we were able to complete three to four steps. Currently, we have methyl (E)-3-(5-methyl pyrazine-2-yl) acrylate which can be produced in up to a 5 g scale.

We plan to continue the research until early May, and then offer our knowledge to another interested student who will continue to work to synthesize the target of interest. In the future, we plan to optimize our condition and synthesis route to obtain TOI1. Also, a graduate student will take over the project upon completion of the synthesis of TOI1 to work towards the other derivatives such as TOI4 and ETS1.

LIST OF REFERENCES

1. What is Multiple Myeloma? (2016). *American Cancer Society*. Retrieved on Feb 13 from <https://www.cancer.org/cancer/multiple-myeloma/about/what-is-multiple-myeloma.html>
2. Cea, M., Cagnetta, A., Gobbi, M., Patrone, F., Richardson, P. G., Hideshima, T., & Anderson, K. C. (2013). New Insights into the Treatment of Multiple Myeloma with Histone Deacetylase Inhibitors. *Current Pharmaceutical Design*, 19(4), 734–744.
3. Handy, D. E., Castro, R., & Loscalzo, J. (2011). Epigenetic Modifications: Basic Mechanisms and Role in Cardiovascular Disease. *Circulation*, 123(19), 2145–2156.
4. Kim, H.-J., & Bae, S.-C. (2011). Histone deacetylase inhibitors: molecular mechanisms of action and clinical trials as anti-cancer drugs. *American Journal of Translational Research*, 3(2), 166–179.
5. Atadja, P. Development of the pan-DAC inhibitor panobinostat (LBH589): successes and challenges (2009). *Cancer Letters*. 280 (2), 233-241.
6. Andreu-Vieyra, C. V., & Berenson, J. R. (2014). The potential of panobinostat as a treatment option in patients with relapsed and refractory multiple myeloma. *Therapeutic Advances in Hematology*, 5(6), 197–210.
7. S. Ropero, M. Esteller (2007). The role of histone deacetylases (HDACs) in human cancer. *Molecular Oncology*, 1, 19–25.
8. FDA approves Panobinostat for some patients with multiple myeloma (2015). *National Cancer Institute*. Retrieved on Feb 14 from <https://www.cancer.gov/news-events/cancer-currents-blog/2015/fda-approves-panobinostat>
9. FDA approves Farydak for the treatment of multiple myeloma (2015). *U.S. Food & Drug Administration*. Retrieved on Feb 14 from <http://www.fda.gov/NewsEvents/Newsroom/PressAnnouncements/ucm435296.html>
10. Laubach, Jacob P., Moreau, Philippe, San-Miguel, Jesus, & Richardson, Paul G. Richardson. (2015) Panobinostat for the treatment of Multiple Myeloma. *Clinical Cancer Research*. 4767-4773
11. Dickschat JS, Wickel S, Bolten CJ, Nawrath T, Schulz S, Wittmann C. (2010) Pyrazine biosynthesis in *Corynebacterium glutamicum*. *European Journal of Organic Chemistry*. 2010:2687–95.

12. Barrow, James C., Zhi-Qiang Yang (2013). Pyrazinyl Amide T-type Calcium Channel Antagonists. Merck & Co. Inc.
13. Wzorek et al. (2013). Synthesis, characterization and antiproliferative activity of β -aryl- δ -iodo- γ -lactones. *Journal of Molecular Structure*. 1047 (2013) 160–168.
14. CG200745, Potentially Best-in-Class HDAC inhibitor for Solid Tumors. (2012). *CrystalGenomics*. Retrieved on Feb 23 from <http://www.crystalgenomics.com/en/clinical/anticancer.html?ckattempt=1>
15. Sabnam et al. (2013). Histone Deacetylases: A Saga of Perturbed Acetylation Homeostasis in Cancer. *Journal of Histochemistry and Cytochemistry*. 62 (1).
16. Gryder, Berkley E, Quaovi H Sodji, and Adegboyega K Oyelere. (2012). Targeted Cancer Therapy: Giving Histone Deacetylase Inhibitors All They Need to Succeed.” *Future Medicinal Chemistry* 4.4: 505–524.
17. Ruijter et al. (2003). Histone deacetylases (HDACs): characterization of the classical HDAC family. *Journal of Biochemistry*. 737–749.